THEORETICAL AND EXPERIMENTAL INVESTIGATION OF THE PLASMA SOURCE WITH ARGON RF BARRIER DISCHARGE AT ATMOSPHERIC PRESSURE

V.Yu. Bazhenov[1], V.V. Tsiolko[1], V.M. Piun[1], R.Yu. Chaplinskiy[2], A.I. Kuzmichev[2]

[1]Institute of Physics NAS of Ukraine, Kyiv, Ukraine;
[2]National Technical University of Ukraine "KPI", Kyiv, Ukraine

E-mail: chapok86@ukr.net

Glow characteristics of capacitive radio frequency discharge with isolated electrodes in atmospheric pressure argon in low-current α and high-current γ modes are determined experimentally and calculated by the hybrid hydrodynamic model. Comparative analysis of obtained experimental data and simulated spatio-temporal distributions of concentrations of discharge plasma electrons and heavy species, mean energy of electrons in the RF barrier discharge enabled interpretation of the discharge structure peculiarities in low-current α, α-γ transition and high-current γ modes.

PACS: 52.80.Pi, 61.30.Hn, 81.65.-b

INTRODUCTION

In the past decade the capacitive RF atmospheric pressure glow discharges were widely used in many applications, including sterilization, surface and exhaust treatment, and even for creation of layers for liquid crystal alignment [0]. Advantages of such discharge type are low ignition voltage and ability to create dense uniform plasma in relatively large volume. As in the case of low pressure discharges, atmospheric pressure ones can exist in two modes – low-current α mode, and high-currents γ mode. Transition from α to γ mode occurs in result of "breakdown" of space charge layers in α mode, which in the case of bare metal electrodes leads to contraction of the discharge, and at subsequent voltage growth and sufficient power of energy source may lead to arcing [0]. The use of dielectric barriers allows stabilization of the discharge in γ mode.

However, the experimental studies of RF discharges at atmospheric pressure mostly appeared to be difficult due to poor reproducibility of the results obtained in different systems because of small discharge gap and high value of the electric disturbance.

Good quantitative predictions could be achieved by the theoretical methods on the basic of the hybrid models of discharge and comparing results with experimental data. But theoretical investigations of the RF discharge are mostly dedicated to the helium discharge with bare metal electrodes. At the same time, there are many applications where argon discharge is more preferable.

The present paper reveals experimental and theoretical investigation of structure and composition of argon RF discharge with the isolated electrodes at atmospheric pressure in low, transition and high current modes.

1. EXPERIMENTAL SET UP AND METHODS

The discharge cell was powered by RF generator through the capacitive divider C1-C4 (Fig. 1), which, together with output stage of matching circuit, provided the discharge power supply in current source regime, that is, with pre-determined values of the discharge current density. The RF voltage waves at the divider input and at both the discharge electrodes were recorded and processed for determining values of current through the discharge cell and voltage at the discharge gap U_d between the barriers. All measurements were done at argon flow rate 3 l/min.

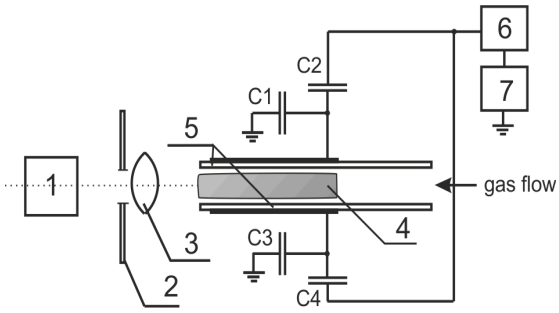

Fig. 1. Experimental setup. 1 – DSLR camera/CCD-spectrometer SL40-2-1024USB; 2 – diaphragm; 3 – lens; 4 – plasma in discharge gap; 5 – dielectric barriers; 6 – impedance matching unit; 7 – RF generator (13.56 MHz)

For observation of transverse structure of the discharge emission, optical setup using CCD spectrometer with 25 x 200 μm input slit was used. The discharge gap imaging with 1:1 magnification was done by means of quartz achromatic lens with 150 mm focal length and 15 mm diameter. At that, the lens aperture was reduced in direction across the discharge gap by slit having 5 mm width. Such setup provided diffraction-limited resolution of about 50 μm FWHM in the image plane and about 1 cm depth-of-field required for correct observation of the emission from the whole discharge thickness. Spatial spectrum distributions were obtained by the spectrometer movement in direction across the discharge image with about 10 μm precision.

The main method of our theoretical investigation was hybrid hydrodynamic model. It is relatively simple in comparison with the full Boltzmann equation and fast in

comparison with PIC methods which need much more amount of resources and additional approximation for modeling the discharges at atmospheric pressure.

This model was based on the continuity equations for concentration of electrons and their energy in discharge gap, at that coefficients in these equations were calculated by solving Boltzmann equation in two-term approximation. Heavy particles were treated by the diffusion equation, and electric filed strength was calculated by the Poisson equation. Joule heating, fluid motion of heavy species and influence of impedance matching box were neglected. The system of partial differential equations was solved numerically. Plasma-chemistry consists of reactions between e, Ar, Ar* (4s configuration, which contains a resonant and a metastable states), Ar_2*, Ar^+, Ar_2^+. At that, Ar^* value is mainly contributed by concentration of long-lived metastable state $1s_5$ [3]. We chose to treat them as a single compound state Ar^*.

The reactions cross-sections and rate coefficients are obtained from literature [3, 4] and from the Boltzmann solver BOLSIG+ [0].

2. RESULTS AND DISCUSSION

By comparing of the measured and simulated V-I characteristics (Fig. 2) it is shown that simulated results are in a good agreement with experimental data. Practically linear part on the experimental V-I characteristic corresponds to the low current α – mode with the current density $J_d \approx 36…74$ mA/cm^2. Part with the negative differential resistance corresponds to the transition α - γ mode and the extreme points on experimental curve represent operation in the high current γ – mode.

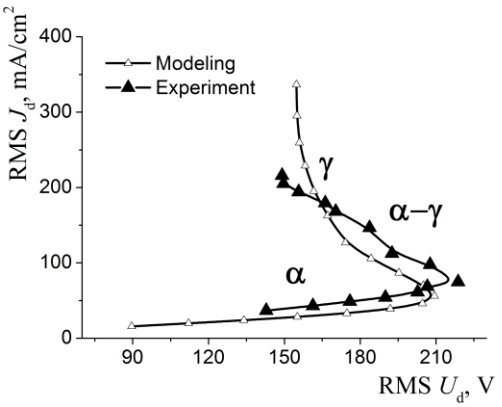

Fig. 2. Experimental and simulated V-I characteristics of the RF discharge

Behavior of spatial distribution of the emission intensity of argon lines with 750.4 and 811.5 nm wavelength in the low-current, transition and high-current modes is shown in Figures 3 and 4, respectively. Emission line at 750.4 nm originates from $2p_1 – 1s_2$ transition. At that, $2p_1$ level is mainly excited by direct electron hit from Ar atom ground state (13.5 eV excitation threshold). And the line at 811.5 nm is emitted by transition from $2p_9$ level to $1s_5$ one. The excitation of the $2p_9$ level occurs mainly from $1s_5$ metastable state by electrons with energy ≥ 2 eV. It is due to the following circumstances. Although ratio of the concentrations of metastable atoms to those in ground state is about $10^{-5}…10^{-3}$, at that: 1) maximum cross section value of $1p_9$ level excitation from metastable state $1s_5$ exceeds by about an order of magnitude the cross section value of excitation from ground state [6]; 2) relative quantity of electrons with energy ≥ 2 eV is essentially bigger than that of electrons with the energy exceeding excitation threshold of $1p_9$ level from ground state (≈ 14 eV). Thus, in first approximation, the emission intensity at 750.4 nm is proportional to the plasma density n_e, and that at 811.5 nm – to population of metastable atoms $1s_5$. However, at interpretation of spatial dependencies of emission intensity shown in Figs. 3, 4 one should draw an attention to the following. Excitation rate of Ar states ($2p_1$, $2p_9$) by electron hit is $K \sim n_e \cdot N \int f(\varepsilon)\sigma(\varepsilon)d\varepsilon$, where: N is concentration of Ar atoms in ground or metastable state; f(ε) is electron energy distribution function; σ(ε) is excitation cross section of this level. As it is shown by the calculation results (Fig. 6), time-averaged energy of plasma electrons reaches maxima in near-electrode regions, and has minimum value in a midpoint of the discharge gap. Due to that, spatial distributions of emission intensity of Ar lines at 750.4 nm and 811.5 nm in our case are functions of not just the plasma density, but also of mean electron energy ε. As a result, spatial distributions of emission of these lines are $\sim n_e \cdot \varepsilon$ and only approximately represent spatial distributions of the plasma density and the concentration of metastable argon atoms. At the same time, positions of the maxima of emission intensity spatial distribution actually coincide with plasma generation zones. Indirect evidence of this is given by a fact that in all discharge glow modes positions of emission intensity maxima for the lines at 750.4 and 811.5 nm practically coincide.

As one can see from the Figs. 3 and 4, in the low-current mode maxima of spatial intensity distributions for both lines are located closer to the discharge gap center, which corresponds to zones of plasma generation and electron heating under electric field action. In the transition and the high-current modes the maxima are shifted towards the surfaces of dielectric plates, which is considered to be due to the discharge transition to γ mode with consequent enhancement of influence of γ electrons on the processes of plasma generation and electron heating.

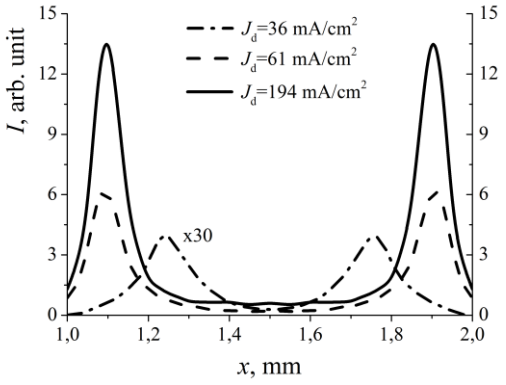

Fig. 3. Experimental time-averaged spatial distribution of Ar 750.4 nm line emission intensity across the discharge gap at different J_d

One can also see difference in the shapes of emission intensity spatial distributions in these figures. In case of Ar 750.4 nm line, the emission is practically

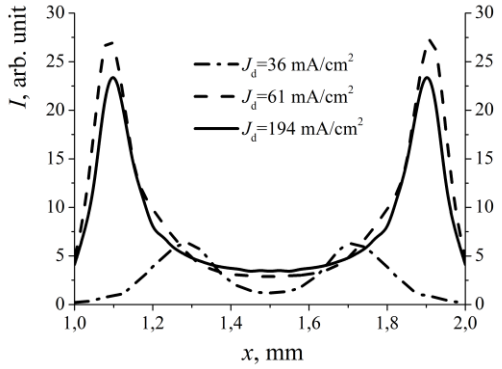

Fig. 4. Experimental time-averaged spatial distribution of Ar 811.5 nm line emission intensity across the discharge gap at different J_d

absent in a middle of the discharge gap, whereas Ar 811.5 nm line emission has noticeable value. It is due to the following: 1) lifetime of $2p_1$ state is essentially shorter than that of $1s_5$ state ($\approx 2\cdot10^{-8}$ s and $\approx 10^{-6}$ s [7], respectively); 2) excitation of $2p_1$ level is performed by direct electron hit from ground state with threshold energy of the process $\approx$ 13.5 eV, and excitation of $2p_9$ state-by electrons with $\geq$ 2 eV from $1s_5$ metastable state. Due to that, Ar ($2p_1$) atoms quickly radiate in the plasma generation zone in vicinity of the discharge electrodes, and electron energy in a middle of the discharge gap is insufficient for excitation of ($2p_1$) state. Although argon atoms in $1s_5$ state originate in the same zone, as Ar ($2p_1$), they can diffuse to mid-part of the discharge gap due to essentially longer lifetime and can be efficiently excited there to $2p_9$ state due to lower excitation threshold. For the same reason, the maxima of Ar 750.4 nm line emission intensity are somewhat narrower than those of 811.5 nm line.

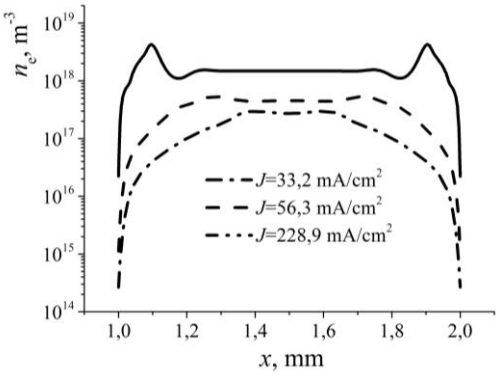

Fig. 5. Simulated time-averaged spatial distribution of electron concentration n_e across the discharge gap at different J_d

Three modes of RF discharge operation can be also distinguished at calculated time-averaged electrons concentration n_e in Fig. 5. In α – mode maxima of electron concentration are situated inside the discharge gap. These maxima correspond to the locations where the most ionization processes by highly energetic electrons take place.

By comparison of time-averaged distribution of electron concentration across the discharge gap calculated here and in the [8], one can see that the width of space charge sheath in barrier RF discharge in α –mode are wider (0.74 mm) than in the argon RF discharge with the bare metal electrodes (0.47 mm) with the same J_d, length of discharge gap and frequency of applied voltage. The difference is caused by the electrons accumulated on the dielectric barrier surface. At the same time, in high current γ – mode the space charge width becomes equal. This is due to the nature of the γ – mode which is similar to DC discharge where the width of space charge are defined by the distance from the cathode to the negative glow which depends mostly on a product of the pressure value and the discharge gap dimension, rather than on material of the cathode.

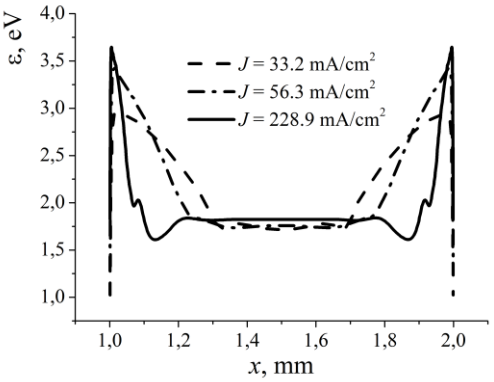

Fig. 6. Simulated time-averaged spatial distribution of electron energy ε across the discharge gap at different J_d

Mean electron energy distributions across the discharge gap (see Fig. 6) show that in all discharge modes a zone with the low energy ($\varepsilon \approx$ 1.8 eV) electrons exists in the middle of discharge gap. Zones with "hotter" electrons are located near the discharge electrodes. At the discharge glow transition from α to γ mode, width of these zones decreases, and mean electron energy in these zones grows up.

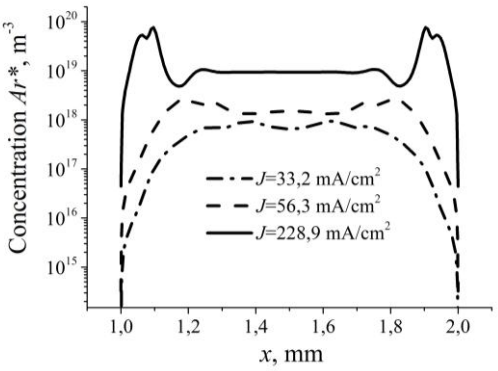

Fig. 7. Simulated time-averaged spatial distribution of Ar concentration across the discharge gap at different J_d*

Behavior of time-averaged concentration of the metastable argon atoms Ar* and excimer molecules Ar_2* across the discharge gap demonstrates similar spatial distribution (Figs. 7, 8). At that, in all discharge modes Ar_2* concentration exceeds that of Ar* by a factor of 5…10. Metastable atoms reach highest density inside the discharge gap in α–mode, whereas in γ-mode their maxima are located at about 100 μm from the electrodes. Note that in transition mode four sharp maxima are situated closer to the dielectric surface (although it is difficult to see them in these log scale graphs). The two maxima, which are situated closer to the dielectric, correspond to the regions with high energy secondary electrons, and the second pair mainly corresponds to the electrons heated due to electric field influence. In the "deep" γ-mode two peaks situated near the dielectric surface merge into the single one.

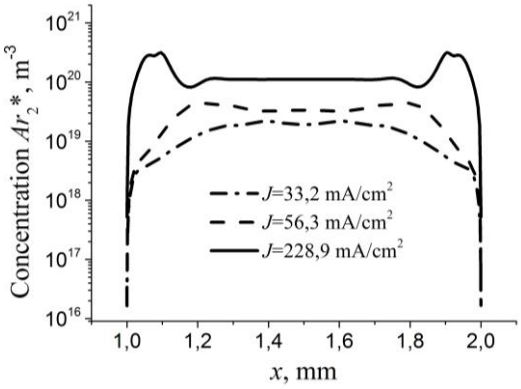

Fig. 8. Simulated time-averaged spatial distribution of Ar_2 concentration across the discharge gap at different J_d*

It should be noted that at low pressures free electron path is longer than the discharge gap, and the metastable profile has its maximum in the center of discharge gap. The profile is then the diffusion dominated [9]. At atmospheric pressure, this diffusion plays a minor role, as it is shown in [0].

REFERENCES

1. V.Yu. Bazhenov et al. // *Problems of Atomic Science and Technology. Series"Plasma physics" (19)*. 2013, № 1, p. 177-179.
2. J.J. Shi and M.G. Kong // *Journal of Applied Physics (97).* 2005, p. 023306-1 - 023306-6.
3. N. Balcon, G.J.M. Hagelaar, and J.P. Boeuf. Numerical Model of an Argon Atmospheric Pressure RF Discharge // *IEEE Transactions on Plasma Science.* 2008, № 5, v. 36.
4. Xi-Ming Zhu and Yi-Kang Pu // *J. Phys. D: Appl. Phys.* 2010, v. 53, p. 015204-015221.
5. G.J.M. Hagelaar and L.C. Pitchford // *Plasma Sources Sci. Technol.* 2005, v. 14, p. 722-733.
6. John B. Boffard, Garrett A. Piech, Mark F. Gehrke, L.W. Anderson, Chun C. Lin // *Physical Review A*. 1999, v. 59, p. 2749-2663.
7. Benedikt Niermann. *The role of metastable atoms in radio-frequency micro-plasma jet discharges operated at atmospheric pressure*. Bohum, 2012, p. 57-73.
8. Farouk Tanvir, Farouk Bakhtier, Gutsol Alexander, Fridman Alexander // *Plasma sources Sci. Technol*. 2008, v. 17, p. 0350151-15.
8. Marisa Roberto, Helen B. Smith, and John P. Verboncoeur // *IEEE Transactions on Plasma Science.* 2003, v. 31, p. 1292-1298.

Article received 23.09.2014

ТЕОРЕТИЧЕСКОЕ И ЭКСПЕРИМЕНТАЛЬНОЕ ИССЛЕДОВАНИЯ ПЛАЗМЕННОГО ИСТОЧНИКА С ВЧ-БАРЬЕРНЫМ РАЗРЯДОМ В АРГОНЕ ПРИ АТМОСФЕРНОМ ДАВЛЕНИИ

В.Ю. Баженов, В.В. Циолко, В.М. Пиун, Р.Ю. Чаплинский, А.И. Кузьмичёв

Характеристики емкостного высокочастотного разряда с изолированными электродами в аргоне атмосферного давления в слаботочном α- и сильноточном γ-режимах установлены экспериментально и рассчитаны с помощью гибридной гидродинамической модели. Сравнительный анализ полученных экспериментальных данных и смоделированных пространственно-временных распределений концентраций электронов и тяжелых частиц, средней энергии электронов в ВЧ-барьерном разряде дал возможность интерпретировать особенности структуры разряда в слаботочном α, переходном α-γ и сильноточном γ-режимах разряда.

ТЕОРЕТИЧНЕ ТА ЕКСПЕРИМЕНТАЛЬНЕ ДОСЛІДЖЕННЯ ПЛАЗМОВОГО ДЖЕРЕЛА З ВЧ-БАР'ЄРНИМ РОЗРЯДОМ В АРГОНІ ПРИ АТМОСФЕРНОМУ ТИСКУ

В.Ю. Баженов, В.В. Ціолко, В.М. Піун, Р.Ю. Чаплинський, А. І. Кузьмичов

Характеристики ємнісного високочастотного розряду з ізольованими електродами в аргоні атмосферного тиску в слабкострумовому α- та сильнострумовому γ-режимах встановлено експериментально та розраховано за допомогою гібридної гідродинамічної моделі. Порівняльний аналіз одержаних експериментальних даних та змодельованих просторово-часових розподілів густин електронів та важких часток, середньої енергії електронів у ВЧ-бар'єрному розряді дав можливість інтерпретувати особливості структури розряду в слабкострумовому α, перехідному α-γ та сильнострумовому γ-режимах розряду.